

# Generative Memorize-Then-Recall framework for low bit-rate Surveillance Video Compression

Yaojun Wu, Tianyu He, Zhibo Chen, *Senior Member, IEEE*,

**Abstract**—Applications of surveillance video have developed rapidly in recent years to protect public safety and daily life, which often detect and recognize objects in video sequences. Traditional coding frameworks remove temporal redundancy in surveillance video by block-wise motion compensation, lacking the extraction and utilization of inherent structure information. In this paper, we figure out this issue by disentangling surveillance video into the structure of a global spatio-temporal feature (memory) for Group of Picture (GoP) and skeleton for each frame (clue). The memory is obtained by sequentially feeding frame inside GoP into a recurrent neural network, describing appearance for objects that appeared inside GoP. While the skeleton is calculated by a pose estimator, it is regarded as a clue to recall memory. Furthermore, an attention mechanism is introduced to obtain the relation between appearance and skeletons. Finally, we employ generative adversarial network to reconstruct each frame. Experimental results indicate that our method effectively generates realistic reconstruction based on appearance and skeleton, which show much higher compression performance on surveillance video compared with the latest video compression standard H.265.

**Index Terms**—video compression, skeleton, attention, generative adversarial network.

## I. INTRODUCTION

**S**URVEILLANCE systems are widely applied for public safety, daily life, remote management, etc. Video sequences recorded by surveillance systems typically contain moving objects, especially human beings, and usually be used for detecting and recognizing. Considering the massive data generated by surveillance systems should be transmitted or stored, as well as being dealt with intelligent algorithms, urgent demands are imposed on an efficient and intelligent compression scheme.

In general, the goal of the compression algorithm is to achieve a compact representation (bit-stream), from which the original content can be reconstructed in a lossy or lossless manner. Such an autoencoder-like process can be formulated as a Rate-Distortion Optimization (RDO) problem, where bit-rate and distortion (the original content v.s. the decompressed content) are considered in the optimization. Traditional hybrid video coding frameworks [1], [2] (such as MPEG-2 [3], H.264 [4] and H.265 [5]) typically tackle the compression problem with four basic steps: prediction, transform, quantization and entropy coding. In this kind of coding framework,

Zhibo Chen is the corresponding author.

Yaojun Wu and Zhibo Chen are with the CAS Key Laboratory of Technology in Geo-spatial Information Processing and Application System, University of Science and Technology of China, Hefei 230027, China (e-mail: yaojunwu@mail.ustc.edu.cn, chenzhibo@ustc.edu.cn). Tianyu He is with the DAMO Academy in Alibaba Group (e-mail: timhe.hty@alibaba-inc.com).

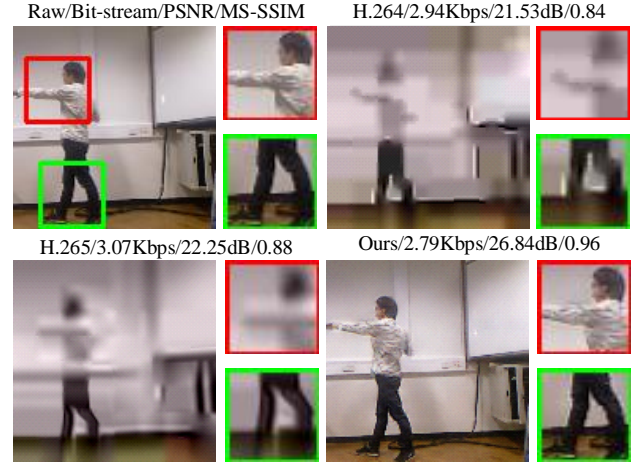


Fig. 1: Visualization of reconstructed video frame compared to the latest video compression standards. It can be observed that our scheme achieves better reconstruction quality while using lower bit-rate.

the redundancy between neighboring frames is mainly decorrelated by block-wise motion compensation. Motion vectors are estimated by searching the best matching block from previous/subsequent frames, which is typically optimized for pixel-level fidelity (e.g., Mean Squared Error).

In the past two years, learning-based image compression has attracted wide attention [6]–[13], while a few research works pay attention to end-to-end learned video compression. Wu *et al.* [14] formulate the video compression as an interpolation problem, and reduce the redundancy in adjacent frames with pre-defined keyframes. Chen *et al.* [15] propose a block-based compression scheme by modeling the spatio-temporal coherence. Lu *et al.* [16] mimic traditional coding frameworks with learning-based components.

However, both traditional coding standards and learning-based schemes are typically optimized for pixel-level fidelity. The inherent structure information inside video signals is not well exploited during the compression process. In this paper, we want to formulate the video compression from the perspective of the semantic-level video decomposition. Our contributions can be summarized as follows.

- We firstly decompose video compression problem as memorizing and recalling processes. Then we propose a new end-to-end video compression framework, named Memorize-Then-Recall (MTR).
- We provide a paradigm for semantic deep video compression. It leverages the success of variational autoencoder

(VAE) and generative adversarial network (GAN). To best of our knowledge, this is the first VAE-GAN based end-to-end video compression framework.

- We verify our MTR framework on video sequences with someone moving around or performing various actions, and achieve superior performance compared with the latest coding standards.

The remainder of this paper is organized as follows. Section II and Section III introduce the related work from the perspective of traditional hybrid coding framework and deep learning based compression, respectively. In Section IV, we formulate our VAE-GAN framework, and detailed description of our model is illustrated in Section V. We will present experimental results in Section VI, and then conclude in Section VII.

## II. BRIEF INTRODUCTION TO TRADITIONAL HYBRID CODING FRAMEWORK

Hybrid Video Coding (HVC) has been widely adopted into most popular existing image/video coding standard like MPEG-2 [3], H.264 [4] and H.265 [5]. Basically, it consists of prediction, transformation, quantization and entropy coding modules. We provided a short explanation of them in the following paragraphs.

*a) Prediction:* Video prediction is introduced to remove the temporal redundancy in traditional video compression. Instead of coding an original pixel value directly, the residual between the original pixel and predicted pixel is encoded after prediction. Prediction typically consists of motion estimation and motion compensation [17]. Motion estimation tries to search through all the possible blocks according to a specific matching criterion (e.g., Sum of Absolute Difference (SAD) or Mean Square Error (MSE)) to find the best matching blocks. While motion compensation directly copies pixels from the matched block in the previously reconstructed frame, and generate a predicted frame.

*b) Transform:* Transform de-correlates coefficients to make them amendable to efficient entropy coding with low-order models. Besides, transform can distribute the signal energy to a few coefficients, which makes it easy to reduce redundancy and correlation. By performing on a reversible linear transform, signal can be transformed into frequency domain such as discrete cosine transform (DCT) and wavelet transform [18].

*c) Quantization:* Quantization is a many-to-one mapping that reduces the number of possible signal values while introducing some numerical errors in the reconstructed signal. Quantization can be performed either on individual values (called scalar quantization) or on a group of values (called vector quantization) [19]. Typically, quantization can significantly reduce the amount of information that required to be transmitted.

*d) Entropy Coding:* In entropy coding, variable-length code and arithmetic coding [40] are common methods. Given source with non-uniform distribution, it can be compressed using a variable-length code where shorter code words are assigned to frequently occurring symbols and longer codes are

assigned to less frequently occurring symbols [20]. Besides, arithmetic coding compresses source by continuously dividing the probability interval of the input symbol.

## III. LEARNING BASED COMPRESSION

### A. Deep Image Compression

In general, deep image compression method jointly trains all modules (transformation, quantization, entropy coding, etc.) with a goal to minimize the length of bit-stream as well as the distortion (e.g., PSNR or MS-SSIM [21]) of the reconstructed image. Among deep compression methods, Toderici *et al.* [6], [22] utilize recurrent neural network (RNN) to compress the image by iteratively feeding the residual information (between reconstructed image and original image) into the RNN-based encoder. In their framework, the compression model can realize variable rates with a single network, without any retraining process. To further improve the compression performance, a spatial adaptive bit allocation method [23] is adopted to apply various bits on different locations for better reconstructed quality.

Besides RNN-based compression methods, variational autoencoder (VAE) also demonstrates its effectiveness in compression. The structure of the VAE-based compression method is firstly proposed in [24], which formulates their framework with non-linear transformation module (convolution with generalized divisive normalization [25]) and relaxed quantization (uniform noise [24]). Then their framework is evolved step by step with soft-to-hard vector quantization [26], conditional entropy probability modeling incorporated with additional hyperprior information [27], and Pixel-CNN based autoregressive context model in entropy modeling [12], [28]. To realize rate control, content-weighted importance-map is utilized in [29].

In addition to utilizing common distortion metric (PSNR or MS-SSIM), adversarial loss [30], [31] and semantic distortion metric (e.g., face verification accuracy distortion [13]) are investigated to improve the reconstructed quality from the perspective of human visual quality or certain task (e.g., face recognition) application.

### B. Deep Video Compression

For video compression task, lots of works leveraging the success of artificial neural networks (ANN) to improve compression performance. They combine ANN with the traditional compression framework to improve the performance of one particular module, such as post-processing [32], mode decision [33], residual coding [34] and entropy coding [35].

In [15], Chen *et al.* propose a learning based video compression method that takes block as the basic processing unit. Wu *et al.* [14] formulate the interpolation based compression method, which removes the redundancy between frames by using interpolation technique to predict frames. Han *et al.* [36] utilize VAE model and introduce two branch encoder to obtain global and local information in the video, which is optimized through pixel-level fidelity. More recently, Lu *et al.* [16] replace traditional video compression modules with neural network components. They first remove the temporal redundancy by predicting frames through the optical flow.

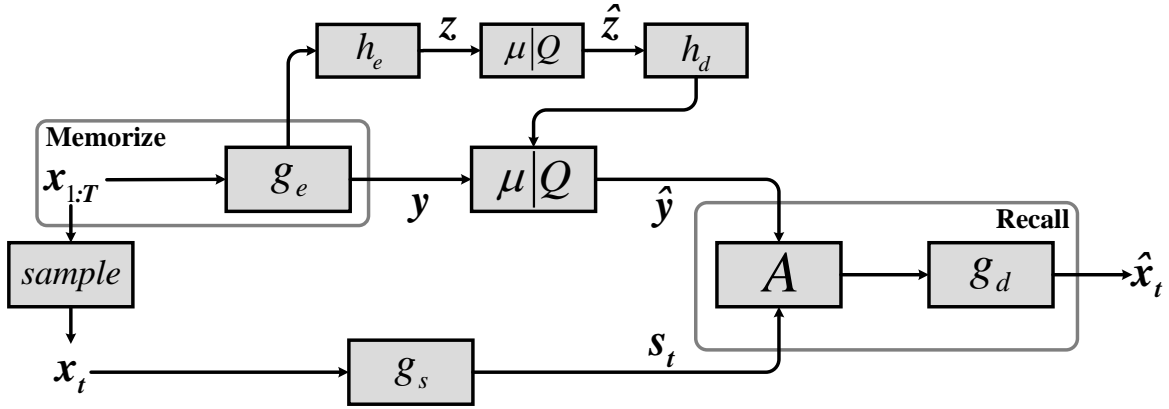


Fig. 2: Diagram showing the operational structure of the video compression model. Boxes represent the operation, while arrows indicate the flow of data. Transformation operations ( $g_e$ ,  $g_d$ ,  $h_e$ ,  $h_d$ ,  $g_s$ ) and attention operation ( $A$ ) are described in section IV. The operation labeled with  $\mu | Q$  represents adding uniform noise during training phase, while it represents quantization and arithmetic coding in testing phase.

After that, they compress the residual information through VAE based network. Rippel et al. [37] consider the redundancy between the optical flow and the residual information. They utilize concatenation to combine these information and feed them into VAE based framework for compression.

#### IV. THE COMBINATION OF VAE AND GAN IN DEEP VIDEO COMPRESSION

Different from traditional hybrid coding frameworks that heuristically optimize each component, we train our framework with end-to-end manner. We leverage the success of variational autoencoder (VAE) [38] in image compression, and combine it with generative adversarial network (GAN) [39]. Detailed information about the combination is described in the following subsections.

##### A. Variational Autoencoder (VAE) based Deep Video Compression

We first solve the video compression problem by VAE. VAE has demonstrated its effectiveness in deep image compression method [12], [27], which even achieves better performance with BPG. Here we expand it into video compression task.

For a Group of pictures (GoP)  $\mathbf{x}_{1:T}$  in video sequence, we employ a parametric transform  $g_e(\mathbf{x}_{1:T}, \phi_{g_e})$  to transform it into latent representation  $\mathbf{M}$ . Since the  $\mathbf{M}$  contains the global information of one GoP, which is similar to the mechanism of human memory, we also call it memory in our paper. The memory information  $\mathbf{M}$  is then quantized to form  $\hat{\mathbf{M}}$ , which will be losslessly compressed by entropy coding techniques (arithmetic coding [40]).

In order to further remove the spatial redundancy in quantized memory  $\hat{\mathbf{M}}$ , we following Ballé *et al.* [27] to utilize hyperprior  $z$  to predict the probability of  $\hat{\mathbf{M}}$  in entropy coding, which is obtained from the hyperprior parametric transformation  $h_e(\mathbf{M}; \phi_{h_e})$ . Then we feed  $\hat{\mathbf{M}}$  into the parametric transformation  $g_d(\hat{\mathbf{M}}, \phi_{g_d})$  to obtain the reconstructed GoP  $\hat{\mathbf{x}}_{1:T}$ .

The goal of our VAE is to approximate the true posterior  $p_{\hat{\mathbf{y}}|\mathbf{x}_{1:T}}(\hat{\mathbf{y}} | \mathbf{x}_{1:T})$  with a parametric variational density

$q(\hat{\mathbf{M}}, \hat{\mathbf{z}} | \mathbf{x}_{1:T})$  by minimizing their Kullback-Leibler (KL) distance over the data distribution  $p_{\mathbf{x}_{1:T}}$ :

$$\begin{aligned} & \mathbb{E}_{\mathbf{x}_{1:T} \sim p_{\mathbf{x}_{1:T}}} D_{KL}[q(\hat{\mathbf{M}}, \hat{\mathbf{z}} | \mathbf{x}_{1:T}) \| p_{\hat{\mathbf{M}}, \hat{\mathbf{z}}|\mathbf{x}_{1:T}}(\hat{\mathbf{M}}, \hat{\mathbf{z}} | \mathbf{x}_{1:T})] \\ &= \mathbb{E}_{\mathbf{x}_{1:T} \sim p_{\mathbf{x}_{1:T}}} \mathbb{E}_{\hat{\mathbf{M}}, \hat{\mathbf{z}} \sim q} \underbrace{\left[ \log q(\hat{\mathbf{M}}, \hat{\mathbf{z}} | \mathbf{x}_{1:T}) - \log p(\mathbf{x}_{1:T} | \hat{\mathbf{M}}) \right]}_0 \underbrace{- \log p_{\hat{\mathbf{z}}|\hat{\mathbf{M}}}(\hat{\mathbf{z}} | \hat{\mathbf{M}}) - \log p_{\hat{\mathbf{z}}}(\hat{\mathbf{z}})}_{D(\text{distortion})} + \text{const.} \\ & \qquad \qquad \qquad \underbrace{\hspace{10em}}_{R(\text{rate})} \end{aligned} \quad (1)$$

We extend the KL distance through Bayes' theorems in (1). The final result contains three parts. The first part corresponds to the joint distribution of the quantized memory  $\hat{\mathbf{M}}$  and quantized hyperprior  $\hat{\mathbf{z}}$ , which is obtained through parametric transformation and adding uniform noise ( as a substitution of quantization [9]). Hence, the first part can be written as follows:

$$\begin{aligned} q(\hat{\mathbf{M}}, \hat{\mathbf{z}} | \mathbf{x}_{1:T}, \phi_{g_e}, \phi_{h_e}) &= \\ & \prod_i \mu(\hat{M}_i | M_i - \frac{1}{2}, M_i + \frac{1}{2}) \times \prod_j \mu(\hat{z}_j | z_j - \frac{1}{2}, z_j + \frac{1}{2}) \\ & \text{with } \mathbf{M} = g_e(\mathbf{x}_{1:T}, \phi_{g_e}), \mathbf{z} = h_e(\mathbf{M}; \phi_{h_e}), \end{aligned} \quad (2)$$

where  $\mu$  denotes the uniform distribution centered on  $M_i$  or  $z_i$ ,  $\hat{z}_i$  denotes the quantized hyperprior and  $\phi$  denotes the corresponding parameters of network. Since the width of the uniform distribution is constant, the result of the first part is equal to zero. Therefore, the first part can be ignored in our loss function.

The second part corresponds to the distortion. In VAE based compression method, this part is always given by Gaussian distribution  $N(\mathbf{x}_{1:T} | \hat{\mathbf{x}}_{1:T}, (2\lambda)^{-1})$ , which is equal to the squared difference between input GoP  $\mathbf{x}_{1:T}$  and reconstructed GoP  $\hat{\mathbf{x}}_{1:T}$ . However, this kind of distortion metric can only measure the distortion from the perspective of pixel level fidelity, which is inconsistent with the human visual system. Hence, we propose to introduce generative adversarial network in VAE framework, which will be detailedly discussed in section IV-B.

The third part represents the total rate of the encoding in VAE-based compression. It includes two items, namely the transmission cost of quantized memory  $\hat{M}$  and quantized hyperprior  $\hat{z}$ . For each element  $\hat{M}_i$  in quantized memory  $\hat{M}$ , we assume it follows a zero-mean Gaussian distribution, in which the standard deviation is predicted by quantized hyperprior  $\hat{z}$  and parametric transform  $h_d(\hat{z}, \theta_{h_d})$ . Therefore, the rate of quantized memory  $\hat{M}$  can be written as follows:

$$p_{\hat{M}|\hat{z}}(\hat{M} | \hat{z}, \phi_{h_e}) = \prod_i (N(0, \sigma_i^2) * \mu(-\frac{1}{2}, \frac{1}{2}))(\hat{M}_i) \quad (3)$$

with  $\hat{\sigma} = h_d(\hat{z}, \theta_{h_d})$ .

As the hyperprior have no prior to predict its density, here we follow Ballé *et al.* [27] utilizing a non-parametric, fully factorized model to predict its probability, which can be seen as follows:

$$p_{\hat{z}}(\hat{z}) = \prod_i (p_{z_i} * \mu(-\frac{1}{2}, \frac{1}{2}))(\hat{z}_i). \quad (4)$$

In the above VAE-based framework, we utilize four parametric transforms ( $g_e$ ,  $g_d$ ,  $h_e$  and  $h_d$ ) to realize the compress and decompress procedures. In theoretical, these parametric transforms can be any parameterized function. In this paper, we utilize artificial neural networks as these transforms, and the detailed structure will be discussed in section V.

### B. Introduce GAN into VAE based Compression Framework

Generative models like Generative Adversarial Networks (GANs) achieve impressive success in lots of tasks recently. In a typical scene, GANs consist of a generator and a discriminator. The core of the GAN is to optimize the minimax game between generator and discriminator. The discriminator aims to determine whether the input is real data, while the goal of the generator is to generate as much realistic data as possible to deceive the discriminator. Such an adversarial training scheme facilitates the generator to yield the generated data with the same distribution as real data. In 2014, Mirza *et al.* [41] further extend GANs into a conditional version, in which some extra information is used as condition when generating data.

Similarly, we treat the process of reconstruction  $g_d$  in VAE as a kind of conditional generation [41], which can be seen in Fig.2. Specifically, for  $t$ -th frame  $\mathbf{x}_t$  in GoP  $\mathbf{x}_{1:T}$ , we first introduce per-frame information  $\mathbf{s}_t$  to help the reconstruction, which is obtained by network  $g_s(\mathbf{x}_t, \phi_s)$ . The local information  $\mathbf{s}_t$  is also called clue in this paper, it helps the reconstruction of each frame. Then we propose recalling attention mechanism  $A(\hat{M}, \mathbf{s}_t, \phi_A)$  to combine the global information  $\hat{M}$  and local information  $\mathbf{s}_t$ , which will be discussed in section V-D. After that, the joint representation is fed into the generator  $g_d$  to obtain the reconstructed frame  $\hat{\mathbf{x}}_t$ .

---

### Algorithm 1 MTR surveillance video compression framework.

---

**Input:**

The input GoP  $\mathbf{x}_{1:T}$ ;

Training: Flag (1 for training and 0 for testing);

**Output:** Reconstructed GoP  $\hat{\mathbf{x}}_{1:T}$  and Bitstream  $B$ .

- 1:  $B \leftarrow []$ ;
  - 2:  $M \leftarrow g_e(\mathbf{x}_{1:T}, \phi_{g_e})$ ;
  - 3:  $z \leftarrow h_e(M, \phi_{h_e})$ ;
  - 4: **if** Training **then**
  - 5:    $\hat{M} \leftarrow M + \mu(-\frac{1}{2}, \frac{1}{2})$ ;
  - 6:    $\hat{z} \leftarrow z + \mu(-\frac{1}{2}, \frac{1}{2})$ ;
  - 7: **else**
  - 8:    $\hat{M} \leftarrow \text{round}(M)$ ;
  - 9:    $\hat{z} \leftarrow \text{round}(z)$ ;
  - 10:  $p_{\hat{M}} \leftarrow h_d(\hat{z}, \phi_{h_d})$
  - 11:  $B \leftarrow \text{Concat}(B, \text{arithmetic coding}(\hat{M}, p_{\hat{M}}))$
  - 12:  $B \leftarrow \text{Concat}(B, \text{arithmetic coding}(\hat{z}))$
  - 13: **for**  $t < T$  **do**
  - 14:    $\mathbf{s}_t \leftarrow g_s(\mathbf{x}_t, \phi_s)$
  - 15:    $B \leftarrow \text{Concat}(B, \text{lossless coding}(\mathbf{s}_t))$
  - 16:   Joint Feature  $F \leftarrow A(\hat{M}, \mathbf{s}_t, \phi_A)$
  - 17:    $\hat{\mathbf{x}}_t \leftarrow g_d(F, \phi_{g_d})$
  - 18:  $\hat{\mathbf{x}}_{1:T} \leftarrow \text{Concate}(\hat{\mathbf{x}}_1, \dots, \hat{\mathbf{x}}_T)$
  - 19: **Return**  $\hat{\mathbf{x}}_{1:T}, B$
- 

For discriminator, it needs to determine as accurately as possible whether the input is real or generated, which can be optimized through the following formula:

$$L_{dis} = \mathbb{E}_{\mathbf{x}_{1:T} \sim p_{\mathbf{x}_{1:T}}} [\log \prod_{t=1}^T p_{d_s}(1 | \mathbf{x}_t)] + \mathbb{E}_{\hat{\mathbf{x}}_{1:T} \sim p_{\hat{\mathbf{x}}_{1:T}}} [\log \prod_{t=1}^T p_{d_s}(0 | \hat{\mathbf{x}}_t)] \quad (5)$$

with  $p_{d_s}(1 | \mathbf{x}_t) = g_{dis}(\mathbf{x}_t, \mathbf{s}_t, \phi_{dis})$ ,  
 $p_{d_s}(0 | \hat{\mathbf{x}}_t) = 1 - g_{dis}(\hat{\mathbf{x}}_t, \mathbf{s}_t, \phi_{dis})$ ,  
 $\mathbf{s}_t = g_s(\mathbf{x}_t, \phi_s)$ ,

where the  $p_{d_s}$  is the probability obtained from discriminator, predicting whether the input frame ( $\mathbf{x}_t$  or  $\hat{\mathbf{x}}_t$ ) is real data (1 for real and 0 for fake). In (5), we assume that the generated frames are independent of each other, and decompose the judgment probability on GoP into the accumulation of judgment probability on each frame. Since the discriminator only judges whether the input is a real frame, we also call it spatial discriminator in this paper.

For generator, it aims to generate frame as closer to real frame as possible. Thus, the loss of the generator can be written as:

$$L_G = -\mathbb{E}_{\hat{\mathbf{x}}_{1:T} \sim p_{\hat{\mathbf{x}}_{1:T}}} [\log \prod_{t=1}^T p_{d_s}(0 | \hat{\mathbf{x}}_t)] \quad (6)$$

with  $\hat{\mathbf{x}}_t = g_d(A(\hat{M}, \mathbf{s}_t, \phi_A), \phi_{g_d})$ .

As described in section IV-A, the distortion part in the VAE optimization function is always defined with square difference, which is inconsistent with the human visual system. In this

part, we utilize the generator loss  $L_G$  as the distortion function in (1), which is more similar to the human visual system compared with the pixel-level fidelity. Based on the above combination of VAE and GAN, we can describe the detailed algorithm of our proposed MTR framework in Algorithm. 1.

In the above VAE-GAN based compression framework, we introduce local information  $s_t$  to improve the generation of each frame  $x_t$ . Theoretically, local information  $s_t$  can be any feature. In this paper, we utilize the pose information (skeleton) obtained from pose estimator as the clue information.

## V. DETAILED FRAMEWORK OF MTR

In section IV, we formulate our video compression framework (MTR) through the combination of VAE and GAN. Here we give a detailed description of our MTR framework. The overall pipeline of the proposed MTR is illustrated in Fig. 3.

For one video sequence, given a GoP  $x_{1:T}$ , we decompose the video content into a global spatio-temporal feature  $M$  (memory) and skeletons  $s_{1:T}$  (clues) for all frames that can be efficiently compressed.

In the encoder, we utilize the Conv-LSTM as the encoder transformation  $g_e$  and abstract the global spatio-temporal feature  $M$  from GoP  $x_{1:T}$ , standing for *memory* to the GoP. It represents appearance for elements that appeared inside GoP, which will be further compressed by quantization and entropy coding ( $h_e$  and  $h_d$ ). For skeletons, they are obtained by the specific pose estimator [43], which served as *clues*. It will be compressed through predictive coding and entropy coding.

In the decoder, the reconstructed spatio-temporal feature  $\hat{M}$  and reconstructed skeletons  $\hat{s}_{1:T}$  can be obtained by corresponding inverse operations in the decompression phase. After that, we introduce a Recalling Attention mechanism  $A$  to implement the recalling process, from which we can attain a feature that combines the information from the  $\hat{M}$  and  $\hat{s}_t$ , describing the appearance with regard to the current frame. We then feed the joint representation into a generator and train it in conjunction with two different discriminators to achieve a realistic frame reconstruction  $\hat{x}_t$ .

Detailed description of each component is in the following subsections.

### A. Memorize over Sequence

Typically, there exist high spatio-temporal correlations between pixels in a video sequence. Existing motion compensation (prediction) method is generally based on the assumption that each block in the current frame is related to a block of a previous/subsequent frame by the motion of objects. Therefore, they de-correlate highly correlated neighboring signal samples by directly copying the corresponding pixels according to estimated motion vectors. However, such pixel-level fidelity can not reflect the inherent structure information of objects.

Hence, we leverage ConvLSTM [44] to model spatio-temporal coherence inside GoP, which aims to obtain global information for one GoP. ConvLSTM utilizes a memory cell  $C_t$  as an accumulator of the state information. The cell is accessed, written and cleared by several self-parameterized

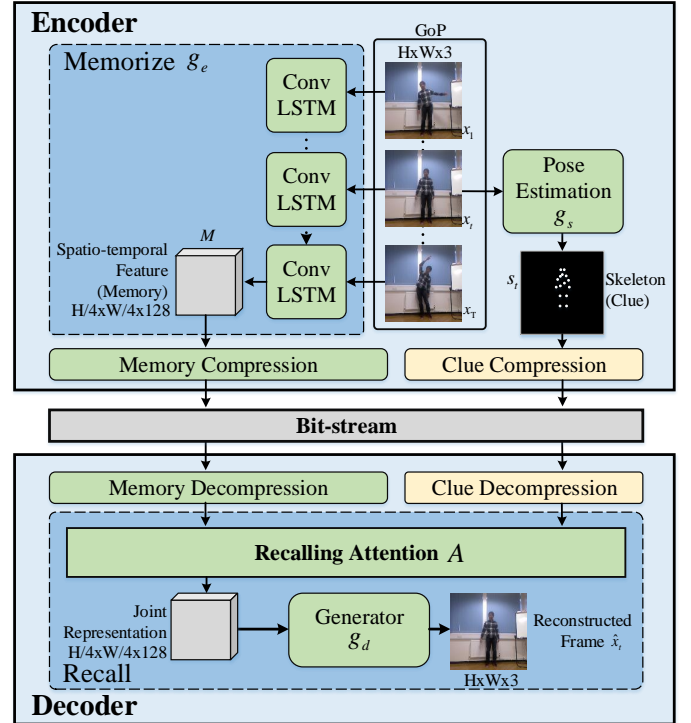


Fig. 3: Memorize-Then-Recall (MTR) Framework. The top and bottom parts demonstrate the encoder and decoder respectively. The size of the feature is denoted as: height×weight×dimension. We jointly train Green modules with the loss defined in section V-E.

controlling gates. Every time a new input comes, its information will be accumulated to the cell if the input gate  $i_t$  is activated. Also, the past cell status  $c_{t-1}$  could be "forgotten" in this process if the forget gate  $f_t$  is on. Whether the latest cell output  $c_t$  will be propagated to the final state  $h_t$  is further controlled by the output gate  $o_t$ . In our method, We utilize frames ( $x_{1:T}$ ) in the GoP as the input of the ConvLSTM, and  $C_t$  is the output of the ConvLSTM. The key equations of ConvLSTM are shown in the following:

$$\begin{aligned}
 i_t &= \sigma(W_{xi} * x_t + W_{hi} * H_{t-1} + W_{ci} \circ C_{t-1} + b_i) \\
 f_t &= \sigma(W_{xf} * x_t + W_{hf} * H_{t-1} + W_{cf} \circ C_{t-1} + b_f) \\
 C_t &= f_t \circ C_{t-1} + i_t \circ \tanh(W_{xc} * x_t + W_{hc} * H_{t-1} + b_c) \\
 o_t &= \sigma(W_{xo} * x_t + W_{ho} * H_{t-1} + W_{co} \circ C_t + b_o) \\
 H_t &= o_t \circ \tanh(C_t),
 \end{aligned} \tag{7}$$

where '\*' denotes the convolution operator and 'o' denotes the Hadamard product.

Specifically, we split a GoP into frames  $\{x_1, x_2, \dots, x_T\}$ . Then we sequentially feed them into ConvLSTM, and final output  $C_T$  is the global spatio-temporal feature for the whole GoP, which is leveraged as memory in our framework.

### B. Memory Compression & Decompression

We utilize the spatio-temporal feature  $M$  as memory to represent appearance for elements that appeared inside GoP. To compress the spatio-temporal feature  $M$ , we firstly apply

a quantization operation. Then, the quantized spatio-temporal feature  $\hat{M}$  is fed into an entropy coder, which further reduces the redundancy with the help of the hyperprior network. Details about the quantization and entropy coding are stated as follows:

a) **Quantization:** As described in (2), we utilize additive uniform noise during the training process. Formally, let  $\mu(a, b)$  denote the uniform distribution on the interval  $(a, b)$ , the quantized spatio-temporal feature  $\hat{M}$  in the training process can be approximated by:

$$\hat{M} = M + \mu\left(-\frac{1}{2}, \frac{1}{2}\right). \quad (8)$$

Note that, such approximation is only performed in the training phase, while we directly apply rounding operation in the testing stage. By performing quantization, the feature memory  $M$  is successfully converted into a limited discrete representation, introducing a great reduction of bit-rate.

b) **Entropy Coding with Hyperprior Modeling:** Context-based entropy coding is a general lossless compression method and commonly used after quantization in traditional coding frameworks. In theory, entropy coding can achieve an optimal solution with a known input probability distribution. However, for media content, the distribution of each sample is different from each other. This motivates some context-based coding scheme that automatically updates probability distribution according to encoded data. Similar to context-based entropy coding adapting to certain content, we introduce a hyperprior network ( $h_e, h_d$ ) to predict the probability distribution for  $\hat{M}$  in (1), which is illustrated in Fig. 4. From Fig. 4, we can see that the bitstream of quantized memory contains two parts, namely the rate for the hyperprior  $z$  and the rate for the quantized memory  $\hat{M}$ . In the memory decomposition phase, the reconstructed spatio-temporal feature  $\hat{M}$  can be obtained by the corresponding inverse operations.

### C. Clue Compression & Decompression

We have already introduce the local information (clue) in (5). In this paper, we utilize skeleton as the clue information for compression. It attends on memory  $M$  and helps the generation of joint representation, which is essential for frame generation in decoder. Therefore, skeleton information is also needed to compress and transmit. In this part, we design a

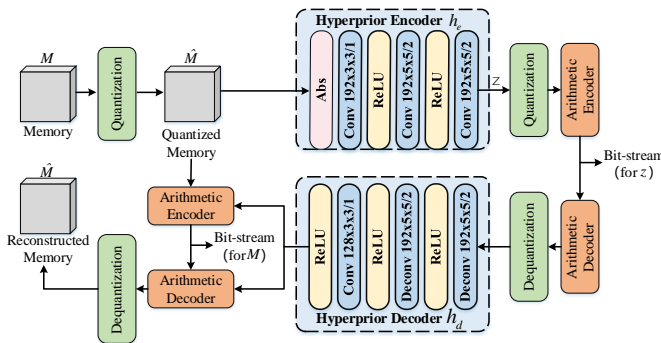


Fig. 4: Our memory compression & decompression. Convolution parameters are denoted as: number of filters  $\times$  kernel height  $\times$  kernel width / stride.

lossless compression method to compress the skeleton. The skeleton  $s_t$  is represented by 18 body nodes and extracted by a pose estimator [43]. For each body node, the coordinates are used to represent the position.

Since there exists continuity between video frames, we first de-correlate them by predicting the coordinate  $s_{t_i}$  of the  $i$ -th node at the current skeleton  $s_t$  with the node in the previous skeleton  $s_{t-1_i}$ . Thereby we can calculate the residual by:

$$res_{t_i} = s_{t_i} - s_{t-1_i}. \quad (9)$$

After that, we use the adaptive arithmetic entropy coding to compress the residual information  $res_{t_i}$ , which can obtain the bit-stream of the clues. In the decompression phase, the reconstructed skeletons  $\hat{s}_{1:T}$  can be computed by the corresponding inverse operations.

### D. Recall from Skeleton

We formulate the combination of the spatial-temporal global information  $\hat{M}$  (memory) and local skeleton information  $\hat{s}_t$  (clue) as an attention procedure in (6). Then the output of the attention is fed into the generator to obtain reconstructed frame  $x_t$ . Here we describe the detailed structure of the recalling attention mechanism  $A$ , the generator  $g_d$  and discriminators.

a) **Recalling Attention:** Attention mechanism has drawn considerable attention from both Natural Language Processing [45], [46] and Computer Vision [47], [48]. Impressively, Vaswani *et al.* [46] introduce self-attention and encoder-decoder attention mechanisms to machine translation, achieving state-of-the-art translation performance. Similarly, Wang *et al.* [47] apply self-attention to the field of computer vision as non-local neural network. The non-local neural network is able to compute the response at a position as a weighted sum of the features at all positions, instead of representing input features with a limited receptive field like convolutional neural networks. Inspired by the success of the aforementioned works, we here present *Recalling Attention*, which mimics the typical recalling process existed in human behaviors. Different from non-local neural network that outputs a global representation of itself, our Recalling Attention allows the skeleton to attend over memory and generate a joint representation that combines the information from both sides. In the following, we describe our recalling attention as a function of *query* and *key-values* pairs. Inspired by the success of the attention mechanism [46],

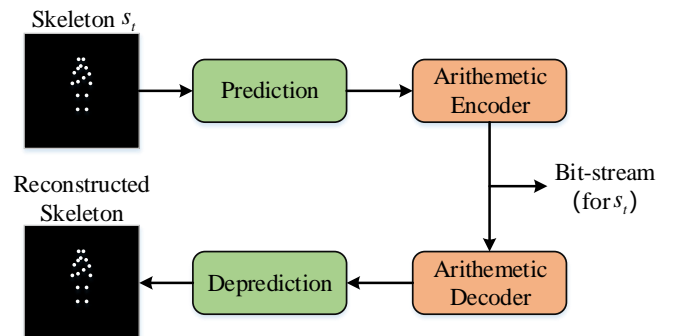


Fig. 5: Our clues compression module.

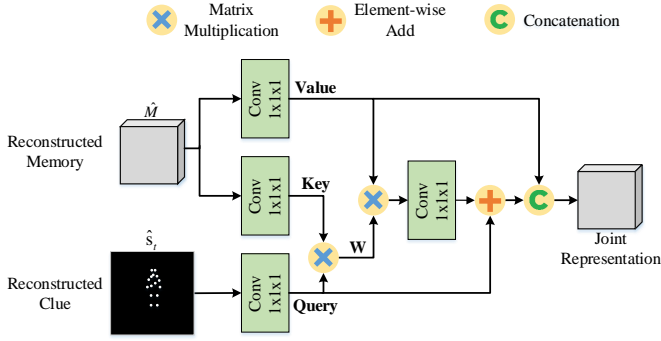


Fig. 6: Our Recalling Attention module.

[47], we here present *Recalling Attention*, which mimics the typical recalling process existed in human behaviors.

Formally, we define a query matrix  $Q$ , a key matrix  $K$  and a value matrix  $V$ . The Recalling Attention  $R(Q, K, V)$  can be formulated as:

$$R(Q, K, V) = [WV^T + Q, V], \quad (10)$$

where  $W$  is a weight matrix to be learned, “+ $Q$ ” represents a residual connection, and  $[\cdot, \cdot]$  indicates concatenation. The convolutional layer is omitted for simplicity. Note that, the weight matrix  $W$  can be learned in different ways [46], [47]. We here adopt the simplest but effective version:

$$W = QK^T. \quad (11)$$

Adapting to our system, as Fig. 6 illustrated, the reconstructed spatio-temporal feature  $\hat{M}$  is regarded as key and value, and the reconstructed skeleton  $\hat{s}_t$  is regarded as the query. Intuitively, our Recalling Attention is computed as a weighted sum over memory, where the weight assigned to each part of memory is computed by the clue with the corresponding part of memory.

**b) Adversarial Generation:** We combine the VAE and GAN by utilizing generator as the transform  $g_d$  and replacing the distortion loss with generator loss  $L_G$  in IV-B. However, the spatial discriminator  $g_{dis_S}$  only independently judges the quality of per frame, lacking the constraint for temporal continuity. To improve the temporal continuity between adjacent generated frames, we following Chan *et al.* [42] and propose additional temporal discriminator  $g_{dis_T}$  for our MTR framework.

The difference between two discriminators can be seen in follows:

- **Spatial Discriminator** ( $g_{dis_S}$ ) takes the skeleton ( $s_t$ ) and the generated or real frame ( $x_t$ ) as input to judge whether the input frame is real or fake. The insight of Spatial Discriminator is to facilitate the generator to yield realistic images conditioned on certain input skeleton.
- **Temporal Discriminator** ( $D_T$ ) takes adjacent skeletons ( $s_t$  and  $s_{t-1}$ ) and corresponding generated or real frames as input to judge whether the input frames are from real video. The goal of the Temporal Discriminator is to ensure the continuity between adjacent generated frames.

Based on the above design, we can modify the optimization function of discriminators with:

$$L_{dis} = L_{dis_S} + L_{dis_T}, \quad (12)$$

where the  $L_{dis_S}$  is already defined in (5). And  $L_{dis_T}$  can be written as:

$$L_{dis_T} = \mathbb{E}_{\mathbf{x}_{1:T} \sim p_{\mathbf{x}_{1:T}}} [\log \prod_{t=1}^T p_{d_T}(1 | \mathbf{x}_{t-1:t})] + \mathbb{E}_{\hat{\mathbf{x}}_{1:T} \sim p_{\hat{\mathbf{x}}_{1:T}}} [\log \prod_{t=1}^T p_{d_T}(0 | \hat{\mathbf{x}}_{t-1:t})] \quad (13)$$

$$\text{with } p_{d_T}(1 | \mathbf{x}_{t-1:t}) = g_{dis_T}(\mathbf{x}_{t-1:t}, \mathbf{s}_{t-1:t}, \phi_{dis_T}),$$

$$p_{d_T}(0 | \hat{\mathbf{x}}_{t-1:t}) = 1 - g_{dis_T}(\hat{\mathbf{x}}_{t-1:t}, \mathbf{s}_{t-1:t}, \phi_{dis_T}),$$

where the  $p_{d_T}$  is the probability obtained from temporal discriminator, predicting whether the input clip is real clip (1 for real and 0 for fake). After that, we can evolve our generator optimization loss by:

$$L_G = -\mathbb{E}_{\hat{\mathbf{x}}_{1:T} \sim p_{\hat{\mathbf{x}}_{1:T}}} [\log \prod_{t=1}^T p_{d_S}(0 | \hat{\mathbf{x}}_t)] - \mathbb{E}_{\hat{\mathbf{x}}_{1:T} \sim p_{\hat{\mathbf{x}}_{1:T}}} [\log \prod_{t=1}^T p_{d_T}(0 | \hat{\mathbf{x}}_{t-1:t})]. \quad (14)$$

With the aid of spatial and temporal discriminators, we can train the generator to learn to generate video reconstructions that satisfy both single-frame authenticity and adjacent-frame continuity. In detail, we base our transformation network  $g_d$  and discriminators on the objective presented in pix2pixHD [49].

#### E. Loss Function for End-to-end Compression Network Training

In section IV and section V-D, we first optimize the compression problem through the variational inference in (1). Then we improve it by replacing the distortion part with generator loss in (6). After that, we utilize additional discriminator to improve the temporal continuity of the adjacent generated frames, which further improve the loss of generator  $L_G$  in (14). Therefore, based on the above formulas, the full loss function of our model can be formulated as follows:

$$\ell = \lambda_{\text{rate}} R + L_G. \quad (15)$$

Based on (15), we further improve the training loss for better reconstruction quality. Following Chan *et al.* [42], we adopt VGG perceptual loss  $\ell_{\text{VGG}}$  by adding it as a part of our distortion loss. In addition, following Ledig *et al.* [50], we introduce the feature matching loss  $\ell_{\text{fm}}$  to improve the training process of our generative model. Therefore, the final training loss for our MTR compression network can be written as:

$$\ell = \lambda_{\text{rate}} R + L_G + \lambda_{\text{VGG}} \ell_{\text{VGG}} + \lambda_{\text{fm}} \ell_{\text{fm}}, \quad (16)$$

where  $\lambda$  balance the importance of each part in loss function. In our experiments, we heuristically set  $\lambda_{\text{rate}} = 1$ ,  $\lambda_{\text{fm}} = 10$  and  $\lambda_{\text{VGG}} = 10$  to train our MTR network.

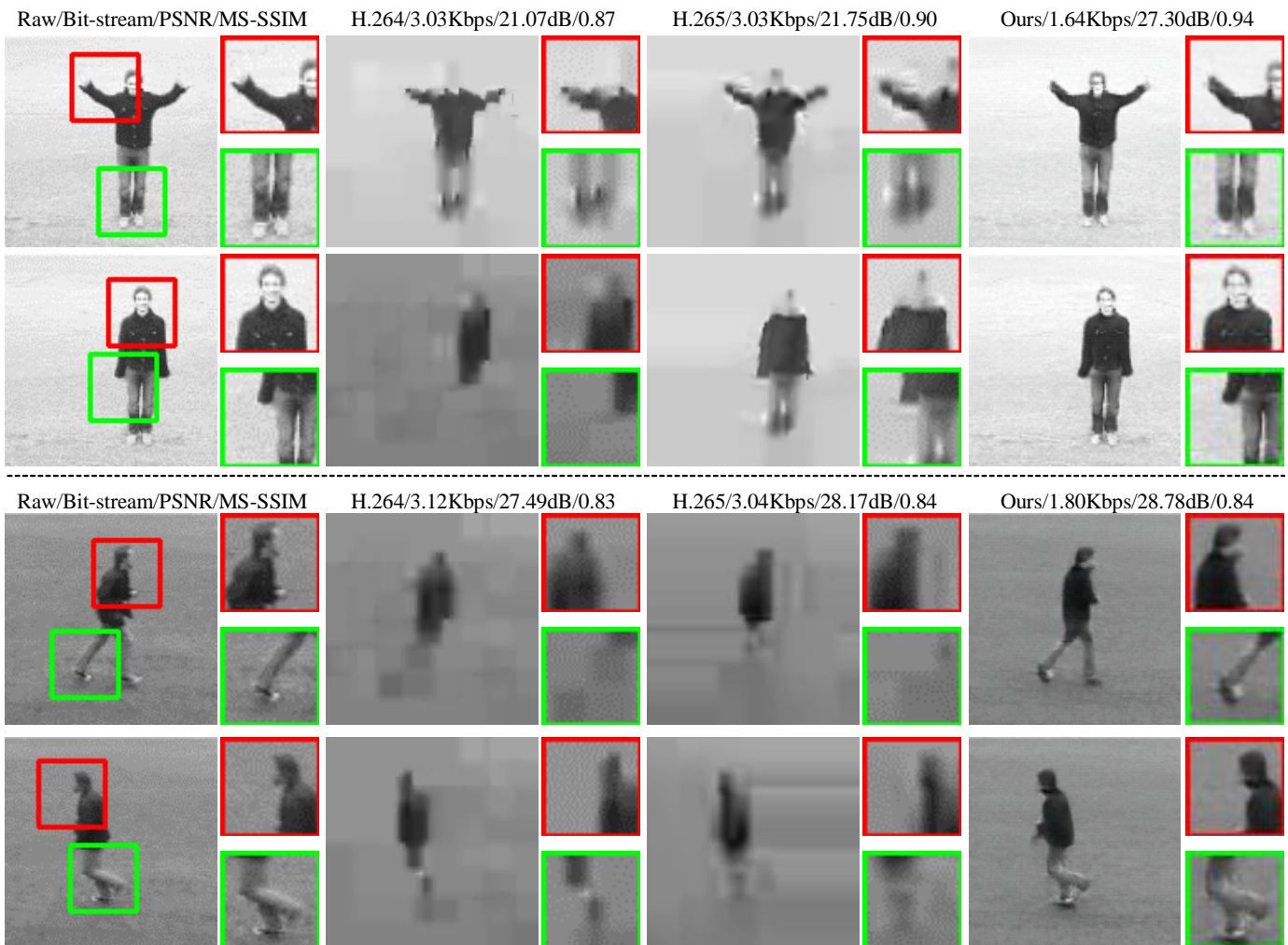


Fig. 7: Comparison between our proposed method and traditional codecs on the test set of KTH dataset.

## VI. EXPERIMENTS

In this section, we first compare our MTR compression performance with traditional video compression codec. Then ablation experiments are conducted to analyze the influence of each module in our framework. Detailed settings about experiments are shown as follows:

*a) Dataset:* We train the proposed video compression framework using KTH dataset [51] and APE dataset [52]. KTH dataset contains six types of different human action classes: walking, jogging, running, boxing, waving and clapping. Each human action is performed several times by 25 actors, yielding 150 video sequences. Each sequence roughly contains 200–800 frames. The spatial resolution of the sequences is  $160 \times 120$ . In our experiment, we randomly divide the KTH dataset into training (130 sequences), validation (12 sequences) and test set (8 sequences) and evaluate the performance on the test set. The APE dataset contains 245 sequences captured from 7 actors. Video sequences of each subject are recorded in unconstrained environments, like changing person poses and moving backgrounds. Similarly, the APE dataset is randomly divided into training (230 sequences), validation (8 sequences) and test set (7 sequences).

*b) Implementation Details:* We utilize the weight of the well-trained model [43] as the initial weight of the pose estimator. The output of the pose estimator is directly fed into the recalling attention module during the training phase. We utilize random crops and random horizontal/vertical flips to realize the data augmentation. The mini-batch size is 4. We use Adam optimizer [53] to update network parameters, in which  $\beta_1$  is set as 0.5 and  $\beta_2$  is 0.999. The initial learning rate is 0.0002. The whole system is implemented based on PyTorch, and it takes about one day to train the model using one NVIDIA GTX 1080Ti GPU.

*c) Metrics:* We adopt PSNR and MS-SSIM [21] to evaluate the performance of our scheme. PSNR is introduced as a common metric to reflect the pixel level fidelity and MS-SSIM indicates the structural similarity. The higher PSNR and MS-SSIM indicate better reconstruction quality. The bit-rate that used for transmission is denoted as Kilobits per second (Kbps) on 25 frames/second (fps).

### A. Comparison with Traditional Codecs

In this subsection, we compare the compression quality of our method with the traditional video codecs, including H.264<sup>1</sup>

<sup>1</sup><https://www.itu.int/rec/T-REC-H.264>

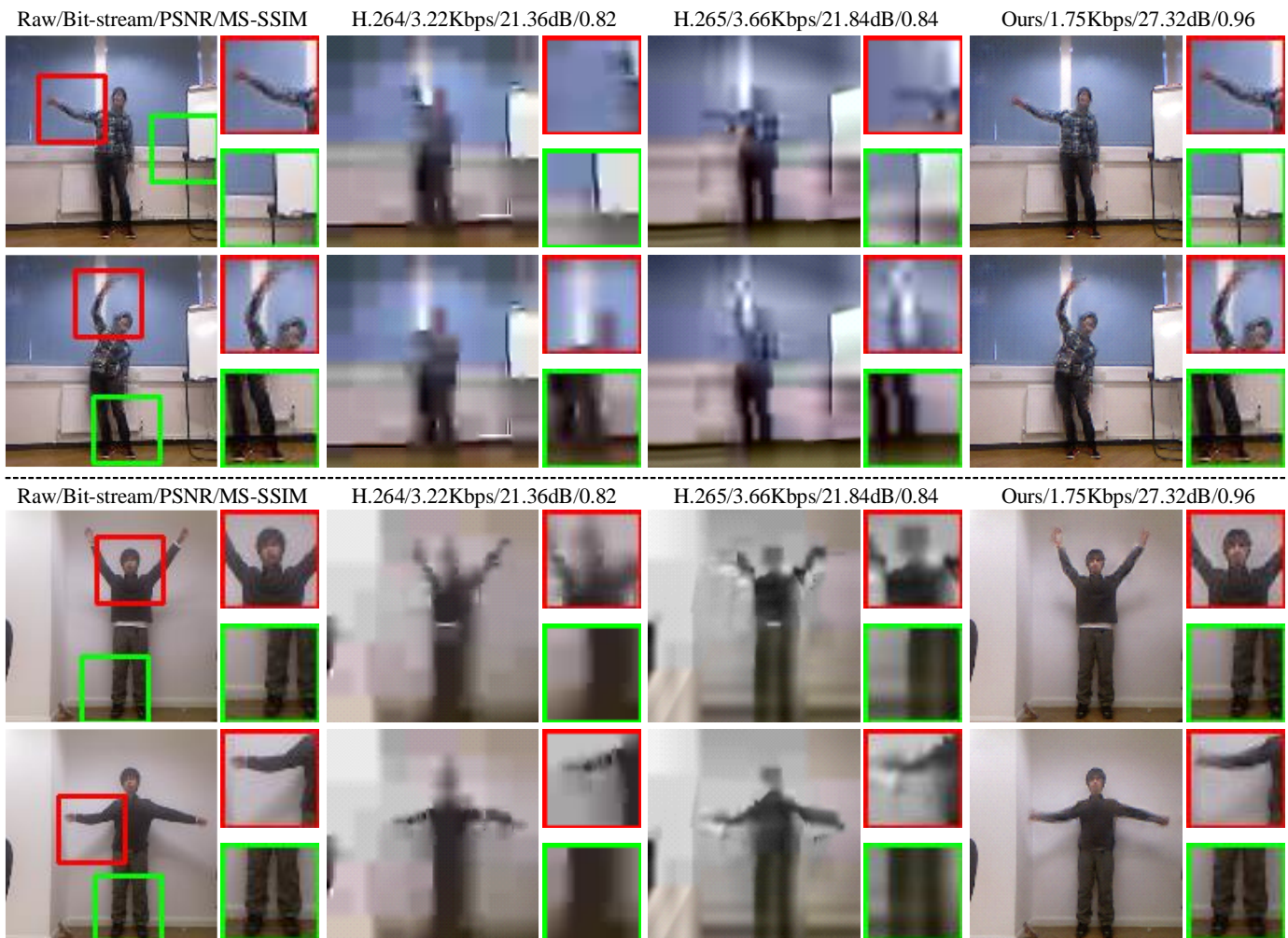


Fig. 8: Comparison between our proposed method and traditional codecs on the test set of APE dataset.

and H.265<sup>2</sup>. For fairness, all codecs use the same GoP size as 10.

Fig. 7 and Fig. 8 visualizes the experimental results on the test set of KTH dataset (top two rows) and APE dataset (bottom two rows), in which the fourth column is generated by our scheme. Note that H.264 and H.265 cannot compress the sequence to a bit-rate lower than about 3 Kbps.

Subjectively, MTR successfully generates video frames with rich details such as grassland and the colorful background. It gets rid of blocking artifacts, and preserve the reality while adapting to the specific pose. We also provide a quantitative evaluation of our framework in Table I, from which we can see that for APE dataset, our scheme significantly outperforms the strong baselines up to 3.61dB with only 56.70% bit-rate. Moreover, our model can be generalized to KTH dataset, which has more complex scenarios (e.g., camera movement), also showing comparable results with the latest video codecs.

Besides testing the quality of the reconstruction, we also test the encoding and decoding time on the same machine (Intel Core i7-8700 CPU / NVIDIA GTX 1080Ti GPU). For a video sequence (300 frames), our model requires 29.67s, while HEVC requires 51.33s. It should be noted that our

TABLE I: Comparison with the latest traditional codecs. Results are averaged on the test set.

	Method	Rate (Kbps)	MS-SSIM	PSNR (dB)
KTH	JM (H.264)	3.96	0.84	25.78
	HM (H.265)	3.54	0.86	26.92
	MTR (Ours)	2.10	0.82	25.68
APE	JM (H.264)	3.27	0.84	23.43
	HM (H.265)	3.21	0.87	24.04
	MTR (Ours)	1.82	0.97	27.65

framework is not technically optimized yet, and it can be further accelerated by model compression or the latest AI chips.

### B. Ablation Experiments

#### a) Ablation on memorizing and recalling mechanisms:

We verify the effectiveness of memorizing and recalling mechanisms by building the framework without memorizing or without recalling respectively. Specifically, the model without memorizing is implemented as directly adopting the first frame as memory, instead of memorizing over the whole sequence. While the model without recalling is implemented as directly concatenating the reconstructed spatio-temporal feature  $\hat{M}$

<sup>2</sup><https://www.itu.int/rec/T-REC-H.265>

TABLE II: Ablation on model architecture. Results are obtained on KTH dataset.

	Rate (Kbps)	MS-SSIM	PSNR (dB)
w/o recalling	2.13	0.78	23.47
w/o memorizing	3.41	0.78	23.48
MonC	2.16	0.82	25.53
MTR (Ours)	2.10	0.82	25.69

and skeletons  $\hat{s}_{1:T}$ , rather than performing Recalling Attention. The experimental results are demonstrated in Table II, from which we can see that the model combined with both techniques (MTR) significantly outperforms two individual baselines.

b) **Variants of attention mechanism:** We conduct different Recalling Attention mechanisms in this part. Specifically, there are two possible attention directions for our Recalling Attention. The first one is “Clues Attend on Memory” (ConM, a.k.a MTR), which is employed in our scheme. As a counterpart, the second one is “Memory Attend on Clues” (MonC). Different with ConM, MonC utilizes  $\hat{s}_t$  as the key and value, and  $\hat{M}$  is regarded as the query. We illustrate the experimental results in Table II. The result shows that MTR achieves better performance than MonC.

## VII. CONCLUSION

In this paper, we propose a Memorize-Then-Recall framework for low bit-rate surveillance video compression by leveraging the inherent structure between frames. With the assistance of the variational autoencoder and generative adversarial network, the proposed framework significantly surpasses the latest coding standards. In the future, we expect to more optimization and plan to extend our framework to more complex surveillance scenarios such as traffic intersections.

## ACKNOWLEDGMENT

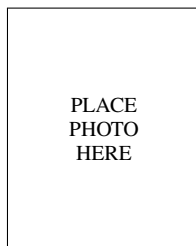
This work was supported in part by NSFC under Grant U1908209, 61571413, 61632001 and the National Key Research and Development Program of China 2018AAA0101400.

## REFERENCES

- [1] A. Habibi, “Hybrid coding of pictorial data,” *IEEE Transactions on Communications*, vol. 22, no. 5, pp. 614–624, 1974.
- [2] R. Forchheimer, “Differential transform coding: A new hybrid coding scheme,” in *Proc. Picture Coding Symp.(PCS-81), Montreal, Canada*, 1981, pp. 15–16.
- [3] ITU-T and I. J. 1, “Generic coding of moving pictures and associated audio information-part 2: video,” 1994.
- [4] T. Wiegand, G. J. Sullivan, G. Bjontegaard, and A. Luthra, “Overview of the h. 264/avc video coding standard,” *IEEE Transactions on circuits and systems for video technology*, vol. 13, no. 7, pp. 560–576, 2003.
- [5] G. J. Sullivan, J. Ohm, W.-J. Han, and T. Wiegand, “Overview of the high efficiency video coding (hevc) standard,” *IEEE Transactions on Circuits and Systems for Video Technology*, vol. 22, no. 12, pp. 1649–1668, 2012.
- [6] G. Toderici, D. Vincent, N. Johnston, S. Jin Hwang, D. Minnen, J. Shor, and M. Covell, “Full resolution image compression with recurrent neural networks,” in *Proceedings of the IEEE Conference on Computer Vision and Pattern Recognition*, 2017, pp. 5306–5314.
- [7] O. Rippel and L. Bourdev, “Real-time adaptive image compression,” in *Proceedings of the 34th International Conference on Machine Learning-Volume 70*. JMLR. org, 2017, pp. 2922–2930.
- [8] M. H. Baig, V. Koltun, and L. Torresani, “Learning to inpaint for image compression,” in *Advances in Neural Information Processing Systems*, 2017, pp. 1246–1255.
- [9] J. Ballé, V. Laparra, and E. P. Simoncelli, “End-to-end optimized image compression,” in *International Conference on Learning Representations (ICLR)*, 2017.
- [10] L. Theis, W. Shi, A. Cunningham, and F. Huszár, “Lossy image compression with compressive autoencoders,” in *International Conference on Learning Representations (ICLR)*, 2017.
- [11] F. Mentzer, E. Agustsson, M. Tschannen, R. Timofte, and L. Van Gool, “Conditional probability models for deep image compression,” in *Proceedings of the IEEE Conference on Computer Vision and Pattern Recognition*, 2018, pp. 4394–4402.
- [12] D. Minnen, J. Ballé, and G. D. Toderici, “Joint autoregressive and hierarchical priors for learned image compression,” in *Advances in Neural Information Processing Systems*, 2018, pp. 10 794–10 803.
- [13] T. He and Z. Chen, “End-to-end facial image compression with integrated semantic distortion metric,” in *2018 IEEE Visual Communications and Image Processing (VCIP)*. IEEE, 2018, pp. 1–4.
- [14] C.-Y. Wu, N. Singhal, and P. Krahenbuhl, “Video compression through image interpolation,” in *Proceedings of the European Conference on Computer Vision (ECCV)*, 2018, pp. 416–431.
- [15] Z. Chen, T. He, X. Jin, and F. Wu, “Learning for video compression,” *IEEE Transactions on Circuits and Systems for Video Technology*, 2019.
- [16] G. Lu, W. Ouyang, D. Xu, X. Zhang, C. Cai, and Z. Gao, “Dvc: An end-to-end deep video compression framework,” *arXiv preprint arXiv:1812.00101*, 2018.
- [17] Z. Chen, J. Xu, Y. He, and J. Zheng, “Fast integer-pel and fractional-pel motion estimation for h. 264/avc,” *Journal of visual communication and image representation*, vol. 17, no. 2, pp. 264–290, 2006.
- [18] Z. Xiong, K. Ramchandran, M. T. Orchard, and Y.-Q. Zhang, “A comparative study of dct-and wavelet-based image coding,” *IEEE Transactions on circuits and systems for video technology*, vol. 9, no. 5, pp. 692–695, 1999.
- [19] N. M. Nasrabadi and R. A. King, “Image coding using vector quantization: A review,” *IEEE Transactions on communications*, vol. 36, no. 8, pp. 957–971, 1988.
- [20] D. Marpe, T. Wiegand, and G. J. Sullivan, “The h. 264/mpeg4 advanced video coding standard and its applications,” *IEEE communications magazine*, vol. 44, no. 8, pp. 134–143, 2006.
- [21] Z. Wang, A. C. Bovik, H. R. Sheikh, E. P. Simoncelli *et al.*, “Image quality assessment: from error visibility to structural similarity,” *IEEE transactions on image processing*, vol. 13, no. 4, pp. 600–612, 2004.
- [22] G. Toderici, S. M. O’Malley, S. J. Hwang, D. Vincent, D. Minnen, S. Baluja, M. Covell, and R. Sukthankar, “Variable rate image compression with recurrent neural networks,” in *International Conference on Learning Representations (ICLR)*, 2016.
- [23] N. Johnston, D. Vincent, D. Minnen, M. Covell, S. Singh, T. Chinen, S. Jin Hwang, J. Shor, and G. Toderici, “Improved lossy image compression with priming and spatially adaptive bit rates for recurrent networks,” in *Proceedings of the IEEE Conference on Computer Vision and Pattern Recognition*, 2018, pp. 4385–4393.
- [24] J. Ballé, V. Laparra, and E. P. Simoncelli, “End-to-end optimization of nonlinear transform codes for perceptual quality,” in *Picture Coding Symposium (PCS)*, 2016. IEEE, 2016, pp. 1–5.
- [25] J. Balle, V. Laparra, and E. P. Simoncelli, “Density modeling of images using a generalized normalization transformation,” in *International Conference on Learning Representations (ICLR)*, 2016.
- [26] E. Agustsson, F. Mentzer, M. Tschannen, L. Cavigelli, R. Timofte, L. Benini, and L. V. Gool, “Soft-to-hard vector quantization for end-to-end learning compressible representations,” in *Advances in Neural Information Processing Systems*, 2017, pp. 1141–1151.
- [27] J. Ballé, D. Minnen, S. Singh, S. J. Hwang, and N. Johnston, “Variational image compression with a scale hyperprior,” in *International Conference on Learning Representations (ICLR)*, 2018.
- [28] J. Lee, S. Cho, and S.-K. Beack, “Context-adaptive entropy model for end-to-end optimized image compression,” *arXiv preprint arXiv:1809.10452*, 2018.
- [29] M. Li, W. Zuo, S. Gu, D. Zhao, and D. Zhang, “Learning convolutional networks for content-weighted image compression,” in *Proceedings of the IEEE Conference on Computer Vision and Pattern Recognition*, 2018, pp. 3214–3223.
- [30] S. Santurkar, D. Budden, and N. Shavit, “Generative compression,” in *2018 Picture Coding Symposium (PCS)*. IEEE, 2018, pp. 258–262.
- [31] E. Agustsson, M. Tschannen, F. Mentzer, R. Timofte, and L. V. Gool, “Generative adversarial networks for extreme learned image compression,”

sion,” in *Proceedings of the IEEE International Conference on Computer Vision*, 2019, pp. 221–231.

- [32] G. Lu, W. Ouyang, D. Xu, X. Zhang, Z. Gao, and M.-T. Sun, “Deep kalman filtering network for video compression artifact reduction,” in *Proceedings of the European Conference on Computer Vision (ECCV)*, 2018, pp. 568–584.
- [33] Z. Liu, X. Yu, Y. Gao, S. Chen, X. Ji, and D. Wang, “Cu partition mode decision for hevc hardwired intra encoder using convolution neural network,” *IEEE Transactions on Image Processing*, vol. 25, no. 11, pp. 5088–5103, 2016.
- [34] T. Chen, H. Liu, Q. Shen, T. Yue, X. Cao, and Z. Ma, “Deepcoder: a deep neural network based video compression,” in *2017 IEEE Visual Communications and Image Processing (VCIP)*. IEEE, 2017, pp. 1–4.
- [35] R. Song, D. Liu, H. Li, and F. Wu, “Neural network-based arithmetic coding of intra prediction modes in hevc,” in *2017 IEEE Visual Communications and Image Processing (VCIP)*. IEEE, 2017, pp. 1–4.
- [36] J. Han, S. Lombardo, C. Schroers, and S. Mandt, “Deep probabilistic video compression,” *arXiv preprint arXiv:1810.02845*, 2018.
- [37] O. Rippel, S. Nair, C. Lew, S. Branson, A. G. Anderson, and L. Bourdev, “Learned video compression,” *arXiv preprint arXiv:1811.06981*, 2018.
- [38] Y. Pu, Z. Gan, R. Henao, X. Yuan, C. Li, A. Stevens, and L. Carin, “Variational autoencoder for deep learning of images, labels and captions,” in *Advances in neural information processing systems*, 2016, pp. 2352–2360.
- [39] I. Goodfellow, J. Pouget-Abadie, M. Mirza, B. Xu, D. Warde-Farley, S. Ozair, A. Courville, and Y. Bengio, “Generative adversarial nets,” in *Advances in neural information processing systems*, 2014, pp. 2672–2680.
- [40] J. Rissanen and G. Langdon, “Universal modeling and coding,” *IEEE Transactions on Information Theory*, vol. 27, no. 1, pp. 12–23, 1981.
- [41] M. Mirza and S. Osindero, “Conditional generative adversarial nets,” *arXiv preprint arXiv:1411.1784*, 2014.
- [42] C. Chan, S. Ginosar, T. Zhou, and A. A. Efros, “Everybody dance now,” *arXiv preprint arXiv:1808.07371*, 2018.
- [43] Z. Cao, T. Simon, S.-E. Wei, and Y. Sheikh, “Realtime multi-person 2d pose estimation using part affinity fields,” in *CVPR*, 2017.
- [44] S. Xingjian, Z. Chen, H. Wang, D.-Y. Yeung, W.-K. Wong, and W.-c. Woo, “Convolutional lstm network: A machine learning approach for precipitation nowcasting,” in *Advances in neural information processing systems*, 2015, pp. 802–810.
- [45] D. Bahdanau, K. Cho, and Y. Bengio, “Neural machine translation by jointly learning to align and translate,” in *International Conference on Learning Representations (ICLR)*, 2015.
- [46] A. Vaswani, N. Shazeer, N. Parmar, J. Uszkoreit, L. Jones, A. N. Gomez, Ł. Kaiser, and I. Polosukhin, “Attention is all you need,” in *Advances in Neural Information Processing Systems*, 2017, pp. 5998–6008.
- [47] X. Wang, R. Girshick, A. Gupta, and K. He, “Non-local neural networks,” in *Proceedings of the IEEE Conference on Computer Vision and Pattern Recognition*, 2018, pp. 7794–7803.
- [48] K. Xu, J. Ba, R. Kiros, K. Cho, A. Courville, R. Salakhudinov, R. Zemel, and Y. Bengio, “Show, attend and tell: Neural image caption generation with visual attention,” in *International conference on machine learning*, 2015, pp. 2048–2057.
- [49] T.-C. Wang, M.-Y. Liu, J.-Y. Zhu, G. Liu, A. Tao, J. Kautz, and B. Catanzaro, “Video-to-video synthesis,” in *Advances in Neural Information Processing Systems (NeurIPS)*, 2018.
- [50] C. Ledig, L. Theis, F. Huszár, J. Caballero, A. Cunningham, A. Acosta, A. Aitken, A. Tejani, J. Totz, Z. Wang *et al.*, “Photo-realistic single image super-resolution using a generative adversarial network,” in *Proceedings of the IEEE conference on computer vision and pattern recognition*, 2017, pp. 4681–4690.
- [51] I. Laptev, B. Caputo *et al.*, “Recognizing human actions: a local svm approach,” in *null*. IEEE, 2004, pp. 32–36.
- [52] T.-H. Yu, T.-K. Kim, and R. Cipolla, “Unconstrained monocular 3d human pose estimation by action detection and cross-modality regression forest,” in *Proceedings of the IEEE Conference on Computer Vision and Pattern Recognition*, 2013, pp. 3642–3649.
- [53] D. P. Kingma and J. Ba, “Adam: A method for stochastic optimization,” *arXiv preprint arXiv:1412.6980*, 2014.



**Michael Shell** Biography text here.

**John Doe** Biography text here.

**Jane Doe** Biography text here.